Recombination processes in Yb-activated ZnS

H. Przybylińska, K. Świątek, A. Stąpor, A. Suchocki, and M. Godlewski
Institute of Physics, Polish Academy of Sciences, aleja Lotników 32/46, PL-02-668 Warsaw, Poland
(Received 6 March 1989)

The occurrence of Yb ions in two charge states (trivalent and divalent) in ZnS is proved with use of the photostimulated electron-paramagnetic-resonance technique. Yb^{2+} is found to form a deep hole-trap center with energy level located at 1.65 ± 0.05 eV below the bottom of the ZnS conduction band. Efficient Yb^{3+} intrashell luminescence is observed under excitation in the region of the valence band to Yb^{2+} photoionization transition. Indirect recombination of a deep Yb-bound exciton with energy transfer to the $4f$ shell of Yb^{3+} is proposed to explain the photoluminescence excitation spectrum. Tentative assignment of the observed broad emission band with the maximum at 10 800 cm^{-1} to direct Yb-bound excitation recombination is suggested.

I. INTRODUCTION

Interest in the studies of emission processes in Yb-doped semiconductors has been stimulated by the prospective application of these materials as a basis for near-infrared-light–emitting diodes and semiconductor lasers. Since Yb^{3+} has only one excited term ($^2F_{5/2}$), located at approximately 10 000 cm^{-1} above the ground ($^2F_{7/2}$) term, infrared emission can be induced without competition with other radiative transitions within the $4f$ shell (as is the case for other rare-earth ions).

To obtain efficient rare-earth (RE) emission, one should understand and control, if possible, photoluminescence (PL) and electroluminescence excitation mechanisms. The possible excitation channels of RE emission in II-VI compounds were summarized by Brown *et al.*[1] and recently by Boyn.[2] The reviews include the direct excitation of the $4f$ shell as well as a range of indirect processes. Knowledge about these processes and their relative efficiencies is, however, still incomplete. In many cases one cannot even be sure which of them is dominant. ZnS:Yb provides a system which should be less complex as at least one of the excitation channels, i.e., the energy transfer from donor-acceptor pairs (DAP's) to a RE ion which is not associated with the donor or the acceptor, should be ineffective. It is a consequence of the mismatch between the energies of DAP recombination and Yb^{3+} $4f\rightarrow4f$ excitation. By studying this system, we hoped to get better insight into the nature of various excitation mechanisms which are of importance in the case of RE-doped ZnS luminophors.

Yb^{3+} has the $4f^{13}$-electron configuration. The difference between the so-called second and third ionization energies for Yb is reduced, which means that the 2+ energy level can be located in the ZnS forbidden gap. Until now such a situation has been found only for europium in ZnS,[3] also due to the reduction of the Eu III–Eu II energy difference because of the half-filled $4f^7$ shell of Eu^{2+}. The basic understanding of a deep center created by a RE impurity in ZnS and other semiconductors is far less advanced than that of transition-metal-related centers in such compounds. In this paper some properties of the deep Yb-related center in ZnS, such as its ionization parameters and free-carrier–capture cross sections, will be presented. We will also show that the RE-ligand bonds have a partially covalent character. The optical data indicate that the covalency of the bonds affects the efficiencies of different PL excitation (PLE) channels.

The paper is organized in the following way. The electron-paramagnetic-resonance (EPR) and photoluminescence results are presented in Sec. II. In Sec. III A the EPR spectrum of Yb^{3+} is analyzed, which enables us to identify the spectrum as being due to substitutional Yb^{3+} with distant charge compensation. In Sec. III B the photostimulated-EPR (photo-EPR) experiments are discussed and the position of the Yb^{2+} energy level within the ZnS forbidden gap is estimated. In Sec. III C the PL excitation spectrum is discussed. The concept of a RE-trapped exciton is introduced and discussed. The experimental results obtained are summarized in Sec. IV.

II. EXPERIMENT

The photo-EPR experiments were carried out on a standard Bruker B-ER 418s spectrometer. A high-pressure XBO 150 xenon lamp and a set of Carl-Zeiss-Jena interference filters were used for sample illumination. The samples were mounted in an Oxford Instruments ESR-900 continuous-gas-flow cryostat, working in the temperature range 3–300 K. The Yb^{3+} photoluminescence was excited by argon-ion–laser lines. An EMI 9684B type-S1 cooled photomultiplier, an ITHACO model 393 lock-in amplifier, and a double-grating GDM 1000 monochromator were used to measure PL spectra. The excitation spectra were taken using an XBO 150 xenon lamp and a single-grating SPM 2 monochromator. The samples were placed in an Oxford Instruments CF 104 continuous-flow cryostat. The measurements were performed on high-resistivity ZnS:Yb crystals of zinc-blende structure. The crystals were grown by the iodine-transport method, with Li added for charge compensation of the Yb^{3+} ions. The details on the crystals used as

well as on the iodine-transport method can be found elsewhere.[4]

In EPR experiments a characteristic spectrum of $Yb^{3+}(4f^{13})$ was observed at 4 K, as shown in Fig. 1. It consists of a strong central line and two sets of hyperfine-interaction-split lines of ^{171}Yb (nuclear spin $I=\frac{1}{2}$, 14.31% natural abundance) and ^{173}Yb ($I=\frac{5}{2}$, 16.31% abundance) isotopes. The spectrum is isotropic with regard to the line positions; however, a small anisotropy of the linewidth was observed. In addition to Yb^{3+}, the EPR spectrum of Mn^{2+} and photosensitive spectra of Cr^{+} and Fe^{3+} were observed. (Transition-metal impurities, such as Mn, Cr, Fe, and Cu, are typical contaminants of ZnS.) An EPR spectrum of the dominant ZnS acceptors, the so-called A centers,[5] was observed under $h\nu > 2.2$ eV excitation.

The intensity of the Yb^{3+} EPR signal was found to be photosensitive. An illumination of the crystals with light of energies $h\nu > 2.2$ eV resulted in a reduction of the signal intensity. A typical time dependence of the Yb^{3+} signal intensity under such excitation is shown in Fig. 2(a) for $h\nu = 3.5$ eV. At first a slight but rapid enhancement was observed (indicating a nonzero occupancy of the Yb^{2+} state prior to illumination); then a slow quenching followed until equilibrium was reached at a lower intensity than the initial one. After the light was turned off, a small, further decrease occurred. Subsequent illumination of the crystals with $h\nu < 2.2$ eV light led, in turn, to an increase of the Yb^{3+} signal intensity [see Fig. 2(b)]. The kinetics of this increase was measured as a function of incident light energy ($h\nu_2$). From the initial rise the increase rate constant was determined. Before each measurement, a primary $h\nu_1 = 3.5$ eV illumination was applied to ensure the same initial conditions (the sequence of steps is shown in Fig. 2). The spectral distribution of the increase rate constant (C_i) normalized to constant light intensity is shown in Fig. 3. The spectrum consists of three distinct bands, with the first starting at 0.8 eV. For $h\nu_2 > 2.2$ eV up to 2.5 eV the quenching of the Yb^{3+} EPR signal intensity was found to dominate over the increase and the equilibrium intensity was lower than the one under 3.5-eV illumination. At $h\nu_2 = 2.5$ eV no

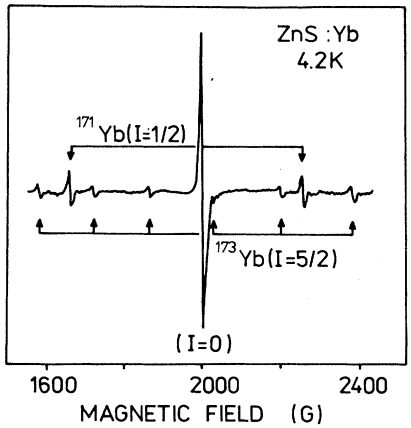

FIG. 1. EPR spectrum of Yb^{3+} in zinc-blende phase of ZnS. Hyperfine-structure lines due to ^{171}Yb and ^{173}Yb are indicated with arrows.

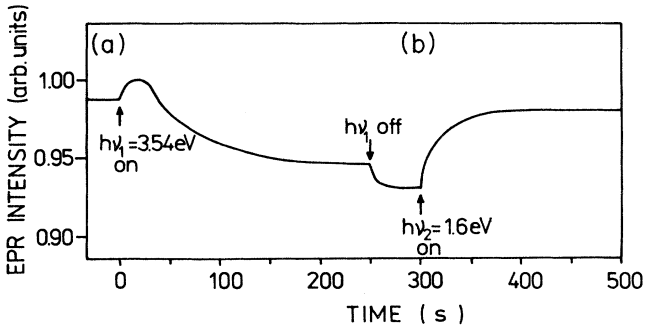

FIG. 2. The sequence of steps in the photo-EPR experiment. Representative kinetics of the intensity of the Yb^{3+} EPR signal under the (a) primary $h\nu_1 = 3.54$ eV and (b) secondary $h\nu < 2.2$ eV illumination are shown.

change of the signal intensity was observed, which means that for this excitation energy the increase and quenching processes are competing and are of equal efficiency. The spectral distribution of the quenching rate constant (C_q) is shown in the inset of Fig. 5.

In photoluminescence measurements a characteristic $^2F_{5/2} \rightarrow {}^2F_{7/2}$ intrashell emission of Yb^{3+} was observed. In the case of an isolated substitutional Yb^{3+} ion in a cubic (T_d symmetry) crystal field, the $^2F_{7/2}$ ground term splits into a lowest-lying Γ_6 doublet, a quartet Γ_8, and a doublet Γ_7, whereas the excited $^2F_{5/2}$ term splits into a lower Γ_6 doublet and a higher Γ_8 quartet. A Γ_8-Γ_6 level reversal for the $^2F_{5/2}$ term of Yb^{3+} was found in InP, which could be related to the partially covalent character of Yb—P bonds.[6] The Γ_8 quartets can be further split into doublets by a crystal field of lower symmetry acting on Yb in complexes. Such an energy scheme of Yb^{3+} should lead to a fairly simple emission spectrum at low temperature when, due to fast thermalization, the emission proceeds only from the lowest excited state of the $^2F_{5/2}$ term. One should, therefore, observe three zero-

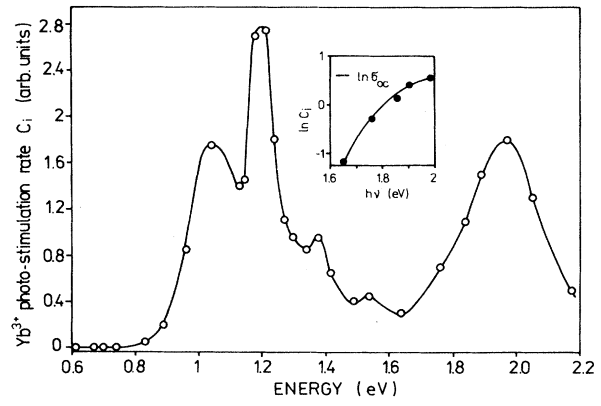

FIG. 3. Spectral distribution of the increase rate constant C_i of the Yb^{3+} EPR signal under illumination. The solid curve is an extrapolation of the experimental points. In the inset the part of the spectrum due to the direct $Yb^{2+} \rightarrow Yb^{3+} + e_{CB}$ photoionization transition is shown with the solid curve representing the fit to the data with formulas (6) and (7) given in the text.

phonon emission lines (ZPL's) for a "cubic center" and four for a "lower-symmetry center" (spread over 100 cm^{-1}, approximately) reflecting the splitting of the $^2F_{7/2}$ ground term. The $^2F_{5/2} \rightarrow {}^2F_{7/2}$ emission spectra of Yb^{3+} measured at three different excitation energies and two different temperatures are shown in Fig. 4. The low-temperature spectra exhibit a more complicated structure than the simple three- or four-ZPL pattern expected for one type of center, as is best seen in the 10 125–10 150-cm^{-1} region. The structure is not due to transitions from higher excited states of the $^2F_{5/2}$ multiplet (so-called "hot" lines). The hot lines appear at about 10 160 cm^{-1} at increased temperatures, as seen in Fig. 4. Moreover, the structure around 10 125–10 150 cm^{-1} depends on excitation energy. Hence we conclude that the observed spectrum consists of at least three superimposed spectra due to different Yb complexes present in the sample. The nature of these complexes remains unknown since, so far, no EPR signal of a low-symmetry Yb^{3+} center in ZnS has been observed. The anisotropic Yb^{3+} spectrum observed by Antipin *et al.*[7] was due to substitutional Yb^{3+} ions in a wurtzite phase of ZnS.

The excitation spectra of Yb^{3+} emission measured at three different temperatures are shown in Fig. 5. The data were obtained for the 10 125-cm^{-1} emission line (which is the dominant one at low temperatures). In the inset we show, for comparison, the spectral dependence of the photoquenching rate of the Yb^{3+} EPR signal. Similar excitation spectra were observed for other emission lines.

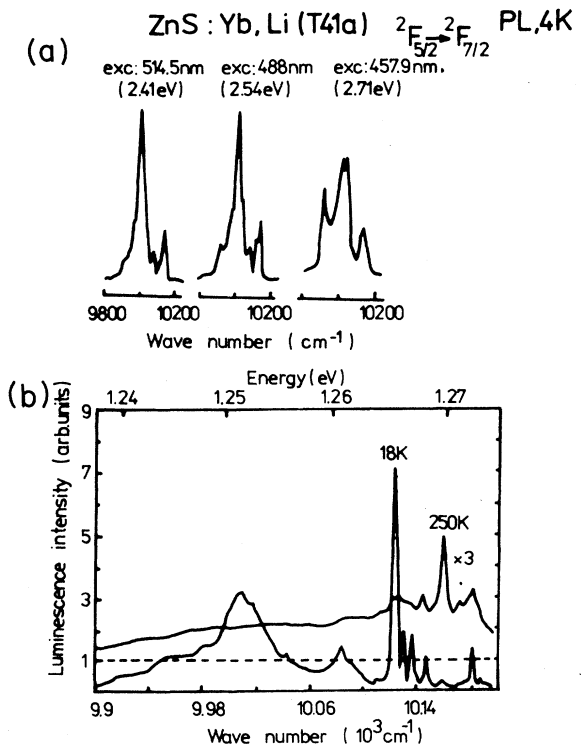

FIG. 4. (a) $^2F_{5/2} \rightarrow {}^2F_{7/2}$ emission of Yb^{3+} in ZnS measured at 4 K for three different excitation energies. (b) High-resolution spectrum of Yb^{3+} emission at 18 and 250 K under 488-nm excitation. The new structure appearing at 250 K is due to so-called "hot" lines.

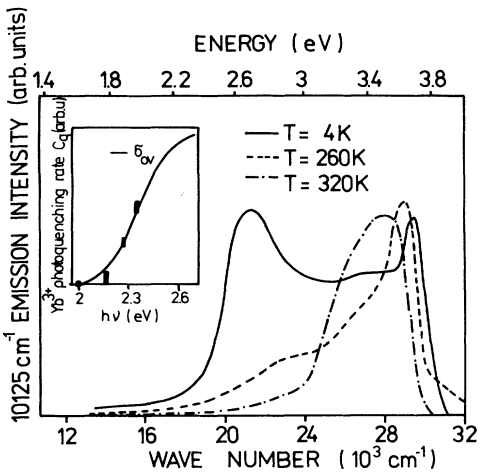

FIG. 5. Excitation spectrum of the 10 125-cm^{-1} emission line of Yb^{3+} measured at 4, 260, and 320 K. In the inset the spectral dependence of the Yb^{3+} photoquenching rate is shown. The solid curve represents the fit to the experimental data with formulas (6) and (7). Typical experimental error is indicated with bars.

III. DISCUSSION

A. Yb^{3+} EPR spectrum

The observed EPR spectrum of Yb^{3+} is that of a Kramers doublet in a cubic crystal field. The splitting of this doublet in a magnetic field can be described by the following effective spin Hamiltonian:

$$\mathcal{H} = g\mu_B \mathbf{B}\cdot\mathbf{S} + \sum_{i=1}^{2} A_i \mathbf{S}\cdot\mathbf{I}_i \ , \tag{1}$$

where, due to the high symmetry of the Yb^{3+} environment, the $\hat{g}$ tensor in the Zeeman term and $\hat{A}_i$ tensors in the hyperfine-interaction terms are isotropic and are replaced by g and A_i constants. The spin-Hamiltonian parameters obtained for the observed spectrum are given in Table I together with those observed for Yb^{3+} in other II-VI compound semiconductor hosts for easy reference.

The attribution of the observed EPR spectrum to Yb^{3+} at a particular site in the ZnS lattice requires some comment, since there are several possible cubic sites (substitutional or interstitial) which a RE ion can occupy.[1,2] In CdTe, for example, a cubic center of Yb^{3+} in an interstitial anion position, surrounded by four Cu_{Cd}(Ag,Au) ions, was identified in EPR.[8] The presence of such a molecule type was also concluded for Er and Tm in ZnSe.[9,10] Another type of cubic center, in which the $(RE)^{3+}$ ion substitutes for the anion and is surrounded by four Cu(Ag,Li) ions on nearest-neighbor cation sites, was also discussed.[11] For these two types of centers the point-charge model of the crystal field predicts the Γ_7 doublet,

with $g(\Gamma_7)=\frac{8}{3}=2.667$, as the ground state of Yb^{3+}, whereas for an isolated Yb^{3+} ion substituting for the cation the ground state is the Γ_6 doublet with $g(\Gamma_6)=\frac{24}{7}=3.429$. The measured g factor of 3.3015 ± 0.0002 is consistent with the one for the Γ_6 doublet; hence we conclude that the observed spectrum is due to substitutional Yb^{3+} in ZnS. Charge compensation by the Li codopant must be rather distant, since it manifests itself only in the small anisotropy of the linewidth, whereas in the case of lithium occupying a nearest-neighbor (NN) cation position the resonant lines would be split and the $\hat{g}$ and $\hat{A}$ tensors would no longer be isotropic. The concentration of such quasi-isolated Yb^{3+} centers can be estimated from the intensity of the EPR spectrum to be about 10^{17} cm^{-3}, i.e., at most a few percent of the Yb concentration in the sample. Unfortunately, the EPR failed to detect Yb^{3+} complexes with close charge compensation, which dominate the PL spectra.

The deviation of the experimentally determined g factor from the $g(\Gamma_6)$ value of 3.4296 (calculated assuming purely ionic bonds) is an indication of considerable covalency effects. Other possible mechanisms which could lead to g-factor deviation, such as the admixture of excited-state wave functions to the ground-state ones induced via crystal field, or Zeeman, terms and/or spin-orbit interaction have been shown by Watts and Inoue to be of less importance.[12] By covalency effects we understand the admixture of ligand wave functions to the $4f$ wave function of a $(RE)^{3+}$ ion occupying a lattice site. The magnitude of this effect can be simply described by the introduction of an orbital-reduction factor k.[8] This is a simplification since, formally, four different orbital-reduction parameters should be introduced to account for the different admixture of π and σ ligand orbitals.[13] The

TABLE I. Spin-Hamiltonian parameters for Yb^{3+} in II-VI semiconductors.

Lattice	g	A^{171} (10^{-4} cm^{-1})	A^{173} (10^{-4} cm^{-1})	Ref.
ZnS:Yb (cubic)	3.3015±0.0002	896±2	246.6±1.5	a
ZnS:Yb (wurtzite)	$g_\parallel=1.242$ $g_\perp=4.400$ $g_{av}=3.347$	$A=330$ $B=1174$	$A=90$ $B=32$	b
CdS:Yb	$g_\parallel=1.1856$ $g_\perp=4.439$ $g_{av}=3.355$	$A=340.5$ $B=1166$		c
	$g_\parallel=2.160$ $g_\perp=2.720$ $g_{av}=2.533$			c
ZnSe:Yb	3.277	903		c
ZnTe:Yb	3.182	860.4	238	d
P-doped	$g_\parallel=1.133$ $g_\perp=4.404$ $g_{av}=3.314$			d
CdTe:Yb	3.117	850	232	c
Cu-doped	2.525	688		c
Ag-doped	2.511	684		c
Au-doped	2.501	684		c
P-doped	3.115	842.5	233.1	e
P-doped	$g_\parallel=0.870$ $g_\perp=4.325$ $g_{av}=3.173$			e e
Li-doped	$g_\parallel=1.834$ $g_\perp=2.832$ $g_{av}=2.499$			
Cu-doped	$g_\parallel=4.734$ $g_\perp=1.152$ $g_{av}=2.533$	$A=1265$		c
Ag-doped	$g_\parallel=4.550$ $g_\perp=1.254$ $g_{av}=2.353$	$A=211$		c
Au-doped	$g_\parallel=5.360$			c

[a]This work.
[b]Reference 7.
[c]Watts and Holton (1968) (Ref. 8).
[d]R. S. Title, Bull. Am. Phys. Soc. **11**, 14 (1966).
[e]R. S. Title, B. L. Crowder, and J. Mayo in *II-VI Semiconducting Compounds*, edited by D. G. Thomas (Benjamin, New York, 1967), p. 1367.

introduction of only one reduction parameter is, however, a justified approximation since only "*xyz*" $4f$ subfunctions, which have lobes pointing towards the ligands, should be sensitive to covalency effects. The orbital-reduction factor for Yb^{3+} in ZnS ($1-k=0.05$), though smaller than that for more covalent II-VI compound semiconductors, is much larger than the value observed in the predominantly ionic crystal CaF_2 ($1-k=0.016$). For other RE ions such relatively large covalency of RE-ligand bonds has not been observed. This is in line with previous suggestions of Watson and Freeman[14] that the $4f$ electrons of Yb are less shielded by outer $5s$ and $5p$ shells from the ligands than $4f$ electrons of other RE ions. The relatively large covalency of the Yb—S bonds can influence considerably the optical cross sections for intra-$4f$-shell and photoionization transitions, as will be discussed in Sec. III B.

B. Yb^{2+} energy level in ZnS

The quenching of the intensity of the Yb^{3+} EPR signal observed under $h\nu>2.2$ eV illumination, together with the simultaneous appearance of an EPR spectrum of hole-populated acceptors, can be explained only by light-induced population of the Yb^{2+} ($4f^{14}$) state. The Yb^{2+} state must, therefore, introduce an energy level into the ZnS forbidden gap. The fact that for $h\nu<2.2$ eV only an increase of the Yb^{3+} signal intensity (i.e., the depopulation of Yb^{2+}) is observed, whereas for higher energies of the incident light both stimulation and quenching of the Yb^{3+} signal (depopulation and population of Yb^{2+}) occur, indicates, moreover, that the Yb^{2+} energy level is located above the middle of the gap ($E_g=3.8$ eV). This means that there is an energy region in which the Yb^{2+} photoionization transition ($Yb^{2+}+h\nu\rightarrow Yb^{3+}+e_{CB}$, where e_{CB} denotes an electron in the conduction band) does not coincide with the complementary Yb^{3+} photoneutralization ($Yb^{3+}+h\nu\rightarrow Yb^{2+}+h_{VB}$, h_{VB} denoting a hole in the valence band), and so by studying the former the Yb^{2+} energy position can be determined. One should bear in mind, however, that light-induced changes in the occupancy of a center observed by means of the EPR technique are not necessarily the result of direct photoionization transitions, but are often caused by indirect processes, e.g., the capture of free carriers generated in the photoionization transitions of other centers present in the crystal.[15] Therefore, the photostimulation and photoquenching spectra usually have a complex nature.

This applies also to the observed photostimulation spectrum of the Yb^{3+} EPR signal shown in Fig. 3. By measuring additionally the spectral dependences of the Cr^+ EPR-signal quenching and Fe^{3+} EPR-signal stimulation, we were, however, able to identify unambiguously all the indirect excitation channels active in our sample. In this way we found that the low-energy bands ($0.8<h\nu<1.6$ eV) observed in the Yb^{3+} photostimulation spectrum are due to the capture of free holes generated in the valence-band–to–acceptor (A) transitions: $A^0+h\nu\rightarrow A^-+h_{VB}$, $Yb^{2+}+h_{VB}\rightarrow Yb^{3+}$. The same bands were found in the Cr^+ photoquenching and Fe^{3+} photostimulation spectra, since the free holes are also captured by Cr^+ ($Cr^++h_{VB}\rightarrow Cr^{2+}$) and partly by Fe^{2+} ($Fe^{2+}+h_{VB}\rightarrow Fe^{3+}$) centers. The latter capture process is much less efficient because the Fe^{2+} center is isovalent in the lattice and the hole is not attracted by a Coulomb potential. The acceptors responsible for these bands are the well-known native defects of ZnS (the zinc vacancy-donor and Cu-donor complexes[16]) and had been populated with holes by the primary $h\nu=3.5$ eV illumination.

By comparing the appropriate increase (C_{Yb}) and decrease (C_{Cr}) rates of the Yb^{3+} and Cr^+ EPR signals measured for $0.8<h\nu<1.6$ eV, the hole-capture cross sections by Yb^{2+} ($\sigma_{p,Yb}$) and Cr^+ ($\sigma_{p,Cr}$) can be estimated. This results from the fact that the kinetics equations describing the decrease of Yb^{2+} occupancy (n_{Yb}) (which is equivalent to the increase of Yb^{3+} occupancy) and the decrease of Cr^+ occupancy (n_{Cr}) under illumination have a similar form:

$$dn_{Yb}/dt=-pv_T\sigma_{p,Yb}n_{Yb}\ , \tag{2a}$$

$$dn_{Cr}/dt=-pv_T\sigma_{p,Cr}n_{Cr}\ , \tag{2b}$$

where p is the concentration of free holes ionized from the acceptors by incident light and v_T is their average thermal velocity in the valence band. After dividing Eq. (2a) by Eq. (2b) we obtain a simple expression,

$$\frac{dn_{Yb}}{n_{Yb}}=\frac{\sigma_{p,Yb}dn_{Cr}}{\sigma_{p,Cr}n_{Cr}}\ , \tag{3}$$

which is easily solved:

$$n_{Yb}(t)/n_{Yb}(0)=[n_{Cr}(t)/n_{Cr}(0)]^{\sigma_{p,Yb}/\sigma_{p,Cr}}\ . \tag{4}$$

Inserting in Eq. (4) the experimentally observed $n_{Cr}(t)/n_{Cr}(0)=\exp(-tC_{Cr})$ time dependence, we obtain

$$n_{Yb}(t)/n_{Yb}(0)=\exp\left[-\frac{\sigma_{p,Yb}C_{Cr}}{\sigma_{p,Cr}}t\right]=\exp(-C_{Yb}t)\ , \tag{5}$$

and, hence, $C_{Yb}/C_{Cr}=\sigma_{p,Yb}/\sigma_{p,Cr}$. The experimental ratio of C_{Yb}/C_{Cr} is about 2, so the hole-capture cross section by Yb^{2+} is of the same order of magnitude as the one by Cr^+, which is approximately 10^{-15} cm^2.[15]

The band in the Yb^{3+} photostimulation spectrum (Fig. 3) starting at 1.6 eV does not appear in the Cr^+ photoquenching and Fe^{3+} photostimulation spectra. This band is due to the direct $Yb^{2+}+h\nu\rightarrow Yb^{3+}+e_{CB}$ photoionization transition. Since in this energy region the two complementary transitions do not coincide, the EPR increase rate constant measured from the initial rise is directly proportional to the optical cross section for the photoionization transition[15] (σ_{oc}, where subscripts c and v denote processes in which free carriers are induced in the conduction and valence bands, respectively). Hence the $C_i(h\nu)$ spectrum yields the $\sigma_{oc}(h\nu)$ dependence and can be fitted with theoretical formulas standardly used for the description of photoionization data, as seen in the inset of Fig. 3. Since for the description of a smooth band observed in a narrow energy range an elaborate theoretical approach is not justified, in our fit we used the simple Kopylov-Pikhtin formula[17]

$$\sigma_{el}(E_{opt},h\nu)\propto(h\nu-E_{opt})^{1/2}(h\nu)^{-3}\ . \tag{6}$$

Because in an ionic compound the change of a center's charge state is accompanied by a relaxation of the lattice around the ionized ion, the Kopylov-Pikhtin formula was extended to account for the electron-phonon interaction in the manner proposed by Langer *et al.*:[18]

$$\sigma_o(h\nu)=\pi^{-1/2}\int_{-\beta}^{\infty} dz\, e^{-z^2}\sigma_{\rm el}(E_{\rm opt},h\nu+\Gamma z)\left[1+\frac{\Gamma z}{h\nu}\right], \tag{7a}$$

$$\beta=(h\nu-E_{\rm opt})/\Gamma\ , \tag{7b}$$

$$\Gamma=\frac{\omega_0}{\omega_{\rm ex}}\left[2(E_{\rm opt}-E_{\rm th})\hbar\omega_0\coth\left[\frac{\hbar\omega_0}{2kT}\right]\right]^{-1/2}, \tag{7c}$$

where ω_0 and $\omega_{\rm ex}$ are the frequencies of phonons coupled to the ground (Yb^{2+}) and excited ($Yb^{3+}+e_{CB}$) states, respectively; $E_{\rm opt}$ is the optical and $E_{\rm th}$ is the thermal ionization energy. From the fit we obtained $E_{\rm opt}=1.76\mp0.02$ eV and $\Gamma=0.1$. The parameter $E_{\rm th}=1.65\mp0.05$ eV was obtained from the threshold of the photoionization band as it is more accurate than the value determined indirectly from the Γ parameter. The experimental data obtained for the complementary Yb^{3+} photoneutralization spectrum are less accurate since under $h\nu>2.2$ eV illumination the stimulation and quenching of the Yb^{3+} EPR signal occur simultaneously. Moreover, in addition to the direct transitions, at least two indirect processes take place, i.e., the capture of holes generated in the $Cr^{2+}+h\nu\rightarrow Cr^{+}+h_{VB}$ transition for $h\nu>2.4$ eV, and the capture of electrons ionized from acceptor centers for $h\nu>2.6$ eV. Hence, only the low-energy wing of the Yb^{3+} photoneutralization band could be observed. The ionization energies obtained from the fit ($E_{\rm opt}=2.25\pm0.10$ eV, $E_{\rm th}=2.15\pm0.20$ eV) are, therefore, less accurate. Their correctness is, however, verified by the fact that the sum of the two thermal ionization energies, as estimated from the thresholds of photo-EPR spectra, gives an energy equal to the energy of the ZnS gap, as expected.

The form of the theoretical formulas applied to fit the experimental data requires some comment. The $Yb^{2+}+h\nu\rightarrow Yb^{3+}+e_{CB}$ transition (from $4f$ states to s-like conduction-band states) should be parity forbidden; however, a better fit was obtained when using formula (6) appropriate for an allowed transition. This is not a very surprising fact since there should be an admixture of ligand wave functions to the $4f$ wave functions of the Yb ion, as deduced from the g-factor value discussed in Sec. III A. This admixture may relax the selection rules and allow the $Yb^{2+}\rightarrow Yb^{3+}$ transition. Apparent effects of covalency of Yb-ligand bonds were observed for the $4f\rightarrow4f$ absorption even in nearly purely ionic crystals such as PbF_2 and CdF_2.[19]

C. PL excitation

As is demonstrated in Fig. 5, the low-energy excitation band of the Yb^{3+} intrashell luminescence correlates with the Yb^{3+} photoneutralization spectrum. This indicates that we are dealing with a new excitation channel of Yb^{3+} intrashell PL, which is not observed for other $(RE)^{3+}$ ions in ZnS. The first step in this process is the ionization of the hole from the $4f$ shell of Yb^{3+} (i.e., the $Yb^{3+}+h\nu\rightarrow Yb^{2+}+h_{VB}$ photoneutralization). To explain the ionization nature of the PL excitation band, one should assume that the subsequent hole recapture on the $4f$ shell proceeds, either directly or indirectly, via the $^2F_{5/2}$ excited state of Yb^{3+}, thus inducing the $^2F_{5/2}\rightarrow{}^2F_{7/2}$ emission.[20]

The observed high quantum efficiency of the above "capture-emission" process indicates that the hole recapture by Yb^{2+} must be very efficient, which is consistent with the photo-EPR results. The hole-capture cross section estimated for Yb centers observed in EPR ($\sigma_{p,Yb}\simeq10^{-15}$ cm^{-2}) is of the same order of magnitude as that for the deep hole trap Cr^{+} and considerably larger than for typical ZnS acceptors.[15] The magnitude of $\sigma_{p,Yb}$ is typical for a Coulomb-attractive center, which confirms our hypothesis that the Yb centers studied in EPR experiments are quasi-isolated and are, in fact, due to Yb complexes, but with the compensating ions (Li^{+}_{Zn}) more distant than at NN cation sites. Such an Yb^{2+}-Li^{+} complex is negatively charged with respect to the lattice (Zn^{2+}-Zn^{2+}) and the hole can be captured by a Coulomb-attractive potential.

There are two experimental facts which cannot be explained within the direct-capture-emission model. One is the strong temperature dependence of the Yb^{3+} PL intensity, as visualized by the experimental data shown in Fig. 6. The 3 ± 1-meV PL deactivation energy estimated from the temperature dependence is much smaller than any ionization energy of hole traps in ZnS. This energy is also in disagreement with the energy balance ($\Delta E\simeq0.9$ eV) for the capture of a free hole directly via the $^2F_{5/2}$ excited term of Yb^{3+}: $Yb^{2+}+h_{VB}\rightarrow Yb^{3+}(^2F_{5/2})+\Delta E$, $Yb^{3+}(^2F_{5/2})\rightarrow Yb^{3+}(^2F_{7/2})+h\nu$. The other puzzling fact is the observation of a broad PL band with the maximum at 10 800 cm^{-1} (shown in Fig. 7); its integrated in-

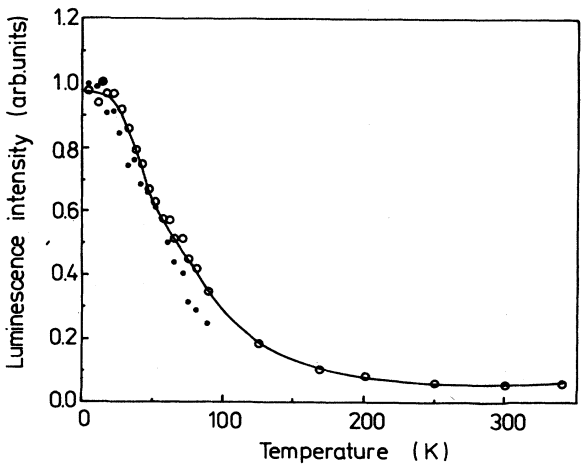

FIG. 6. Temperature dependence of the integrated intensity of Yb^{3+} intrashell emission (denoted by open circles). The temperature dependence of the integrated intensity of the PL band with maximum at 10 800 cm^{-1} is indicated by solid circles. The solid curve is drawn for a 3-meV PL deactivation energy.

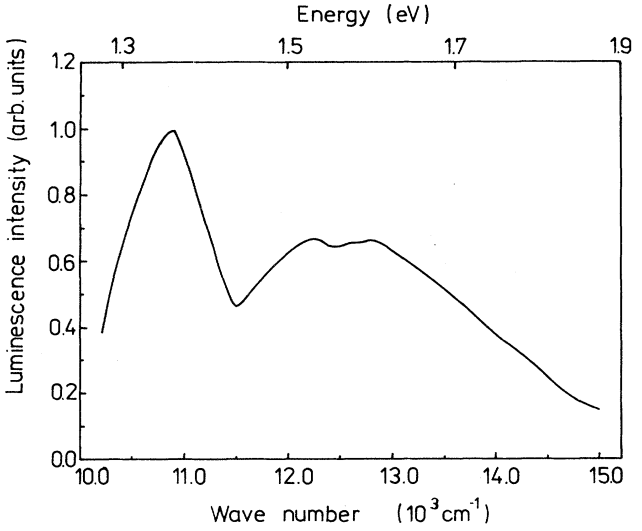

FIG. 7. High-energy part of the Yb-related emission in ZnS.

tensity temperature dependence is similar to the one of the Yb^{3+} intrashell emission (see Fig. 6). The estimated 1.4-eV energy of the zero-phonon line is, however, much lower than the energy of the direct $Yb^{2+}+h_{VB} \rightarrow Yb^{3+}(^2F_{7/2})+h\nu$ transition (2.15 eV).

These two facts can be explained if we assume that the hole ionized from Yb^{3+} to the valence band before being recaptured on the $4f$ shell of Yb^{3+} is first trapped by the Coulomb-attractive potential provided by the compensating lithium ion, thus forming a deep RE-bound exciton (BE). This mechanism would be an analogue of the charge-transfer mechanism of RE excitation reported previously. Broad optical-absorption bands of charge-transfer character were observed for RE ions in bromide solutions,[21] Eu_2O_3 and Yb_2O_3,[22] wide-band-gap oxides,[23] halides,[24,25] oxyhalides,[26] and oxysulfides.[27] Charge-transfer excitation of $(Re)^{3+}$ intrashell emission was shown at first for Sm^{3+} (Ref. 28) and Yb^{3+} (Ref. 27). It was then shown by Garcia *et al.*[29,30] that illumination within the charge-transfer band leads to $4f$-intrashell emission for a series of $(RE)^{3+}$ ions (Nd^{3+}, Sm^{3+}, Dy^{3+}, Ho^{3+}, Er^{3+}, and Tm^{3+}) in wide-band-gap sulfides such as thiogallates. In order to explain the PL excitation mechanism, the formation of a deep bound exciton was postulated.[29–31] In this BE the electron is induced into the $4f$ shell of a RE ion and the photogenerated hole remains trapped on one of the adjacent ligands. The electron-hole pair may recombine indirectly due to energy transfer to the $(RE)^{3+}$ ion, resulting in $4f \rightarrow 4f$ excitation and optical deexcitation.

The experimental results obtained in our studies strongly suggest that we also deal with a deep RE-bound exciton. The electron is strongly localized on the $4f$ shell of Yb^{2+}. The electron binding energy for a quasi-isolated Yb^{2+}_{Zn} center is 1.65 eV (thermal ionization energy) as estimated from the photo-EPR data. The hole is also deeply bound due to the strong hole-attractive potential of the compensating lithium ion. The hole binding energy for the Li_{Zn} center in ZnS is not konwn, but it should be similar to that of the Cu_{Zn} deep acceptor. Although one should expect a reduction of the electron and hole binding potentials for a complex defect, both the electron and hole should be still deeply bound, so that a 2.4-eV exciton binding energy is not surprising. The 1.4-eV emission can thus be associated with the direct BE recombination.

A similar model was proposed recently to explain the Yb^{2+}-related emission in fluorites (SrF_2, BaF_2, and CaF_2).[32,33] In SrF_2:Yb^{2+} an anomalous emission was observed, which was attributed to radiative recombination of the Yb-bound exciton. The exciton consists of Yb^{3+} with a self-trapped electron delocalized over the 12 NN cation sites. Its recombination energy is smaller than the energy of direct $4f^{14} \rightarrow 4f^{13}5d^1$ Yb^{2+} excitation, which reduces the efficiency of energy transfer from the bound exciton to Yb^{2+}. In our case the situation is reversed. The excited $^2F_{5/2}$ term of Yb^{3+} lies below the $(Yb^{2+}+h)$ BE level and fast energy transfer from BE to Yb^{3+} competes with the direct BE recombination.

The observed 3-meV deactivation energy of the BE and Yb^{3+} emissions cannot be directly related to the electron-hole binding energy. The most probable explanation of the low deactivation energy is that the hole ionized from Yb^{3+} is captured first on a hole-excited state of the bound exciton. From this state it can either thermalize down to the lowest BE excited state—followed then by either direct emission or energy transfer—or it can be thermally activated back to the valence band.

At increased temperatures another PLE band dominates, the one characteristic for the excitation of DAP emission in ZnS. As already stated, a large energy mismatch between DAP recombination energy and $4f \rightarrow 4f$ excitation energy ensures that the mechanism responsible for this PLE band cannot be due to energy transfer between unassociated sites. The exact nature of such a mechanism is not clear at the moment. It is however, highly probable that it is due to recombination at DAP-RE complexes (the RE ion is most probably associated with an acceptor), in which the DAP recombination energy is transferred to the nearby Yb^{3+}, followed then by $4f \rightarrow 4f$ emission. It seems, moreover, that the remaining energy can also be emitted radiatively. In fact, we have observed an appropriate broad infrared emission band in the range 11 500–15 000 cm^{-1}, which is expected if such a cooperative process takes place. A similar cooperative recombination has been observed for excitons bound at neutral donors and acceptors (two-electron–two-hole transitions).[34–36]

IV. CONCLUSIONS

In this paper we discuss a novel excitation mechanism of Yb^{3+} intrashell emission in ZnS, which is shown to have a photoionization character ($Yb^{3+} \rightarrow Yb^{2+}+h_{VB}$). The hole ionized from Yb^{3+} in this process is very efficiently recaptured by Yb centers forming a deep Yb-bound exciton. The exciton recombines mainly indirectly due to energy transfer to the $^2F_{5/2}$ excited term of Yb^{3+}, which lies below the $(Yb^{2+}+h)$ BE level, followed then

by $^2F_{5/2} \rightarrow {}^2F_{7/2}$ emission of Yb^{3+}. The observation of a broad emission band with the estimated zero-phonon line at 1.4 eV seems to indicate that direct radiative BE recombination may be also possible. This would give a 2.4-eV binding energy for the Yb-bound exciton.

Another excitation mechanism of Yb^{3+} PL in the DAP excitation region was also observed. We suggest that it is due to DAP recombination at DAP-Yb complexes with a part of the recombination energy transferred to Yb^{3+} and the rest emitted radiatively in a cooperative process.

ACKNOWLEDGMENTS

The authors are indebted to Dr. H. Hartmann, for growing the crystals studied, and Dr. D. Hommel for fruitful discussions. This work has been supported by the Polish Academy of Sciences Program No. CPBP-01-12.

[1]M. R. Brown, A. F. J. Cox, W. A. Shand, and J. M. Williams, Adv. Quantum Electron. **2**, 69 (1974).
[2]R. Boyn, Phys. Status Solidi B **148**, 11 (1988).
[3]M. Godlewski and D. Hommel, Phys. Status Solidi A **95**, 261 (1986).
[4]H. Hartmann, J. Cryst. Growth **42**, 144 (1977).
[5]See, e.g., R. S. Title, in *Physics and Chemistry of II-VI Compounds,* edited by M. Aven and J. S. Prener (North-Holland, Amsterdam, 1967), Chap. 6.
[6]G. Aszodi, J. Weber, Ch. Uihlein, L. Pu-Lin, H. Ennen, U. Kaufmann, J. Schneider, and J. Winscheif, Phys. Rev. B **31**, 7767 (1985).
[7]A. A. Antipin, I. N. Kurkin, and L. A. Shekun, Fiz. Tverd. Tela (Leningrad) **7**, 938 (1965) [Sov. Phys.—Solid State **7**, 753 (1965)].
[8]R. K. Watts, Solid State Commun. **4**, 549 (1966); R. K. Watts and W. C. Holton, Phys. Rev. **173**, 417 (1968).
[9]J. D. Kingsley and M. Aven, Phys. Rev. **155**, 235 (1967).
[10]S. Ibuki, H. Komiya, M. Nakada, H. Masui, and H. Kimura, J. Lumin. **1/2**, 797 (1970).
[11]M. R. Brown, A. F. J. Cox, W. A. Shand, and J. M. Williams, J. Phys. C **4**, 2550 (1971).
[12]R. K. Watts and M. Inoue, Phys. Rev. Lett. **11**, 196 (1963).
[13]K. W. H. Stevens, Proc. R. Soc. London, Ser. A **219**, 542 (1953).
[14]R. E. Watson and A. J. Freeman, Phys. Rev. **133**, A1571 (1964).
[15]M. Godlewski, Phys. Status Solidi A **90**, 11 (1985).
[16]M. Godlewski, Phys. Rev. B **32**, 8162 (1985).
[17]A. A. Kopylov and A. N. Pikhtin, Fiz. Tverd. Tela (Leningrad) **16**, 1837 (1974) [Sov. Phys.—Solid State **16**, 1200 (1975)].
[18]J. M. Langer, in *New Developments in Semiconductor Physics,* Vol. 122 of *Lecture Notes in Physics, Proceedings of the International Summer School held in Szeged, 1979,* edited by F. Beleznay, G. Ferenczi, and J. Giber (Springer, Berlin, 1980), p. 123.
[19]V. J. Abbruscato, E. Banks, and B. R. McGarvey, J. Chem. Phys. **49**, 903 (1968).
[20]A. Stąpor, M. Godlewski, H. Przybylińska, and D. Hommel, J Lumin. **40/41**, 625 (1988).
[21]C. K. Jörgensen, Mol. Phys. **5**, 271 (1962).
[22]C. K. Jörgensen, R. Pappalardo, and E. Rittershaus, Z. Naturforsch. **20a**, 54 (1965).
[23]G. Blasse, J. Chem. Phys. **45**, 2356 (1966).
[24]J. L. Ryan and C. K. Jörgensen; J. Phys. Chem. **70**, 2845 (1966).
[25]J. L. Ryan, Inorg. Chem. **8**, 2053 (1969).
[26]J. Hölsa, Finn. Chem. Lett. **7-8**, 201 (1980).
[27]E. Nakazawa, J. Lumin. **18/19**, 272 (1979).
[28]G. Blasse and A. Bril, Phys. Lett. **23**, 440 (1966).
[29]A. Garcia, F. Guillen, and C. Fouassier, J. Lumin. **33**, 15 (1985).
[30]A. Garcia, R. Ibanez, and C. Fouassier, in *Rare Earths Spectroscopy,* Proceedings of the 1st International Symposium on Rare Earths Spectroscopy Wrocław, Poland, 1984, edited by B. Jeżowska-Trzebiatowska, J. Legendziewicz, and W. Stręk (World Scientific, Singapore, 1985).
[31]K. H. Yang and J. A. Deluca, Phys. Rev. B **17**, 4246 (1978).
[32]D. S. McClure and C. Pedrini, Phys. Rev. B **32**, 8465 (1985).
[33]B. Moine, C. Pedrini, D. S. McClure, and H. Bill, J. Lumin. **40/41**, 299 (1988).
[34]D. G. Thomas and J. J. Hopfield, Phys. Rev. **128**, 2135 (1962).
[35]P. J. Dean, J. D. Cuthbert, D. G. Thomas, and R. T. Lynch, Phys. Rev. Lett. **18**, 122 (1967).
[36]P. O. Holz, B. Monemar, H. P. Gislason, Ch. Uihlein, and P. L. Liu, Phys. Rev. B **32**, 3730 (1985).